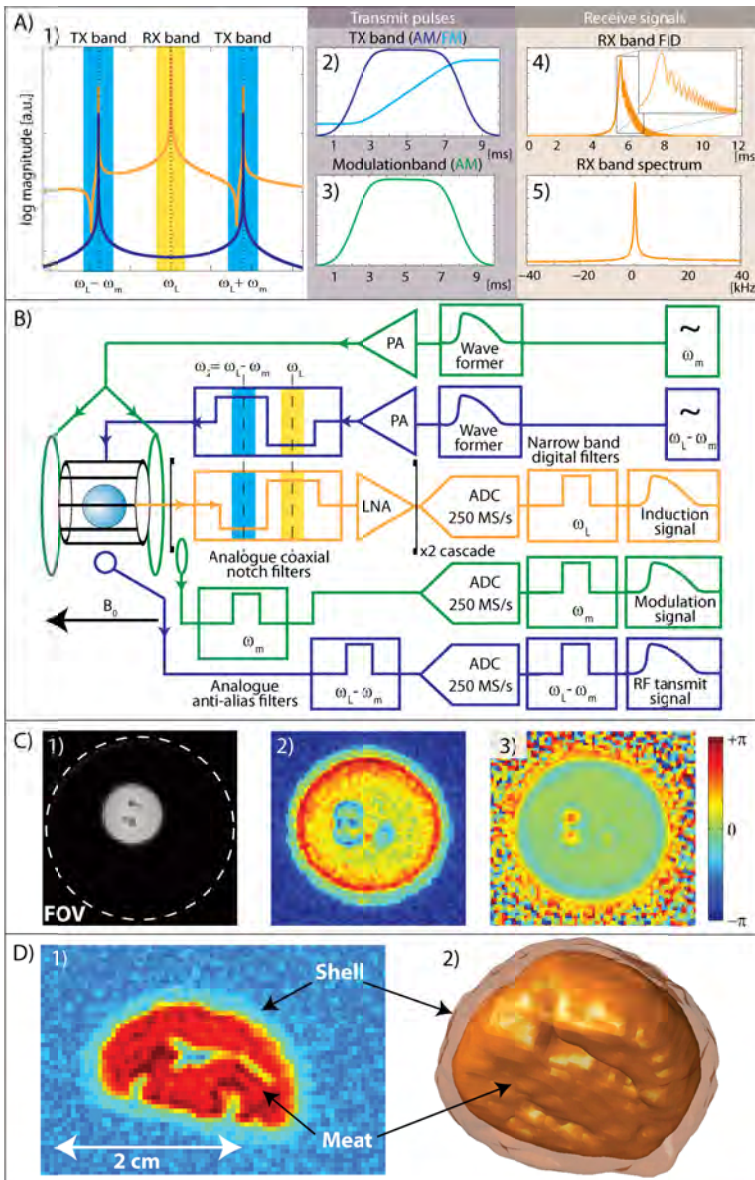


MRI with Sideband Excitation: Application to Continuous SWIFT

David O. Brunner¹, Benjamin E. Dietrich¹, Matteo Pavan¹, and Klaas P. Pruessmann¹
¹Institute for Biomedical Engineering, University and ETH Zurich, Zurich, Zurich, Switzerland



Introduction: Present-day NMR and MRI usually rely on time-interleaved transmission and reception to avoid contamination of the spin signal by the high power excitation pulses. However, actually concurrent excitation and detection would be an interesting capability in general and particularly for studying samples with short coherence times [1, 2, 3, 11]. In conventional setups, this mode of operation would require full isolation of the receivers from the transmit signals, which is very hard to achieve. Even with subtraction schemes (e.g. [4]) the residual transmit signal challenges the linearity and dynamic range of the receivers and the noise floor of the transmitter can diminish the SNR of the weak spin signal. Furthermore, the subtraction approach is hampered even by minimal changes of the coupling situation between the two RF chains, e.g. by heating of the electronics or by any load variation due to motion of the sample or breathing, blood flow, or cardiac dynamics in live imaging targets.

A recently proposed alternative is B_0 modulation [5, 6, 7, 8], which circumvents RF transmission at Larmor frequency by excitation via modulation sidebands and thus permits the use of frequency-selective filtering to prevent transmit signal leakage, receiver saturation and noise injection from power modules. The present work reports the implementation of this approach for MRI, yielding first results of sideband imaging with an adapted SWIFT sequence [5] and additional comprehensive RF monitoring.

Theory & Methods: A time harmonic modulation field (B_m), parallel to B_0 and at a frequency ω_m that is larger than the NMR bandwidth, generates sidebands in the NMR spectrum (A.1). The sidebands occur at $\omega_{n+1} = \omega_L \pm n\omega_m$ and can be regarded as copies of the nuclear resonance at the Larmor frequency (ω_L). RF transmission at the sidebands' frequencies causes spin nutation with an effective $B_{1eff} = \frac{\gamma B_m B_{(n+1)}}{n\omega_m}$, $B_{(n+1)}$ being the RF field at the sideband ω_{n+1} .

Since the frequency bands of the RF transmission signals and received NMR signals are disjoint, the RF transmit signal can be robustly filtered out of the received signal despite remnant coupling into the receive path as long as the system stays linear and electronic intermodulation can be avoided. In the present work the modulation frequency was set to $\omega_m = 2.25$ MHz resulting in reasonable excitation efficiency while separating the two bands sufficiently to protect the receiver gain stages from the transmit signal at the first lower sideband ($\omega_2 = \omega_L - \omega_m$) with coaxial-line notch-filters. The modulation field is generated by a solenoid coil (ϕ 6 cm) and the two linear modes (isolation -18 dB) of a high-pass birdcage coil on a glass substrate (inner ϕ 4 cm) were used for RF transmission and reception. The entirely proton-free setup was placed in the bore of a Philips Achieva 7T system whose gradient system was used to perform center-out trajectories 3D radial image acquisition. Excitation was performed as in the SWIFT technique during an interval with a static gradient, using third-order Houtt-Silver pulses whose amplitude modulation was distributed between the RF (A.2) and the modulation channels (A.3). The corresponding frequency modulation was implemented through the RF channel only. The received signal (A.4) as well as the transmitted signals (A.2&3) at ω_2 and ω_m were recorded by a custom-built spectrometer and used as the basis for a comprehensive signal deconvolution including off-resonance and Bloch-Siegert-shift correction to obtain individual projections (A.5). 3D image data was finally obtained by an iterative gridding reconstruction.

Results: The analogue receive filters had a stopband rejection greater than 60 dB and an passband insertion loss of 1.2 dB, keeping SNR losses low. Fig. C shows reconstructed images obtained from a grape with 0.7 mm isotropic resolution and 8 mT/m read gradient (C.1) as well as a higher-bandwidth

A) 1) Band separation of transmission and reception by modulation 2) recorded RF and 3) modulation pulse, 4) NMR signal, 5) deconvolved spectrum. B) Schematic of the setup. C) Images of a grape; 1) FOV 70 mm, resolution $(0.7\text{mm})^3$, $G_{read}=8\text{mT/m}$. 2) $(0.5\text{mm})^3$ 15mT/m cropped magnitude and 3) phase image. D) Short- T_2 sample (chestnut without cupule). 1) magnitude image res: $(0.55\text{mm})^3$, 29mT/m 2) surface rendering from MR data of the nutmeat and the nutshell.

example with $0.5\text{mm} / 15\text{mT/m}$ plotted in magnitude (C.2) and phase (C.3), which were obtained with 34 dBm of each RF and modulation peak power. Figure D.1 shows a slice of a 0.55 mm resolution scan with 29 mT/m read gradient of a sweet chestnut as a short- T_2 (≈ 1.5 ms and shorter) sample (peak RF and modulation power: 37 dBm). Surface renderings from the 3D data were obtained by thresholding to the intensity of the shell (transparent rendering) and the meat (opaque rendering).

Conclusion: Sideband modulation permits MRI with fully concurrent excitation and detection based on frequency separation. The technique is therefore robust against changes in coupling, loading and the behavior of electronic parts, which hamper subtraction approaches. SWIFT imaging as performed here is one example of a larger class of techniques that may benefit from this capability such as stochastic, Hadamard [9] or time-shifted-sum [10] excitation, and ZTE[11]/BLAST [12]. RF and modulation monitoring offers implicit correction for hardware infidelities such as timing variations and phase drifts, power amplifier compression or temperature drifts and thus helps to achieve very low artifact levels in the reconstructed images as exemplified by C.1. An inherent drawback of the sideband approach is higher required RF power compared to on-resonant excitation. However, this disadvantage is partly countered by the feasibility of larger transmit duty cycles compared to pulsed excitation. Higher excitation efficiency will also be obtained with circularly polarized RF coil heads, transmission on both sidebands and lower modulation frequencies.

[1] Ernst, JMR 1970 [2] Davies, JMR 2001, [3] 2003 Idiyatullin D, JMR 181 2006 [4] Idiyatullin, ISMRM 2011, [5] Krauss Phys Rev A 1986, [6] Kälin, JMR 2003 [7] Michal, J Chem Phys [8] Brunner, ISMRM 2011 [9] Blülich JMR Med Biol 1993 [10] Paff, Adv MR 1992 [11] Weiger, MRM 2011 [12] Hafner, MRI 1994